



THE UNIVERSITY *of* EDINBURGH

Edinburgh Research Explorer

Crystal Structure of SiH₄ under Pressure

Citation for published version:

Degtyareva, O, Martinez-Canales, M, Bergara, A, Chen, X, Song, Y, Struzhkin, VV, Mao, H-K & Hemley, RJ
2007, 'Crystal Structure of SiH₄ under Pressure', *Physical review B*, vol. 76, no. 6, 064123.
<https://doi.org/10.1103/PhysRevB.76.064123>

Digital Object Identifier (DOI):

[10.1103/PhysRevB.76.064123](https://doi.org/10.1103/PhysRevB.76.064123)

Link:

[Link to publication record in Edinburgh Research Explorer](#)

Document Version:

Publisher's PDF, also known as Version of record

Published In:

Physical review B

Publisher Rights Statement:

Copyright belongs to the APS

General rights

Copyright for the publications made accessible via the Edinburgh Research Explorer is retained by the author(s) and / or other copyright owners and it is a condition of accessing these publications that users recognise and abide by the legal requirements associated with these rights.

Take down policy

The University of Edinburgh has made every reasonable effort to ensure that Edinburgh Research Explorer content complies with UK legislation. If you believe that the public display of this file breaches copyright please contact openaccess@ed.ac.uk providing details, and we will remove access to the work immediately and investigate your claim.



Crystal structure of SiH₄ at high pressure

Olga Degtyareva,^{1,2} Miguel Martínez Canales,³ Aitor Bergara,^{3,4} Xiao-Jia Chen,¹ Yang Song,^{1,*} Viktor V. Struzhkin,¹ Ho-kwang Mao,¹ and Russell J. Hemley¹

¹*Geophysical Laboratory, Carnegie Institution of Washington, Washington, DC 20015, USA*

²*Centre for Science at Extreme Conditions, School of Physics, University of Edinburgh, Mayfield Road, Edinburgh EH9 3JZ, United Kingdom*

³*Materia Kondentsatuaren Fisika, Zientzia Fakultatea, Euskal Herriko Unibertsitatea, 644 Posta Kutxatila, 48080 Bilbo, Spain*

⁴*Donostia International Physics Center (DIPC) and Centro Mixto CSIC-UPV/EHU, 1072 Posta Kutxatila, 20080 Donostia, Spain*

(Received 12 March 2007; published 31 August 2007)

The crystal structure of a high-pressure phase of silane (SiH₄), observed between 10 and 25 GPa, is solved using powder synchrotron x-ray diffraction and shown to be of the SnBr₄ type. The phase is an insulating molecular solid with a monoclinic unit cell containing four tetrahedrally bonded molecules, space group $P2_1/c$. *Ab initio* calculations show the SnBr₄-type structure to be favored in this pressure range relative to other recently proposed structures. The fit of the pressure dependence of volume to the Birch-Murnaghan equation of state gives the following parameters at ambient pressure if K'_0 is fixed to 4: $V_0=250(9) \text{ \AA}^3$ and $K_0=7.8(9) \text{ GPa}$ for the experimental data, and $V_0=255(2) \text{ \AA}^3$ and $K_0=6.1(2) \text{ GPa}$ for the data obtained from *ab initio* calculations.

DOI: 10.1103/PhysRevB.76.064123

PACS number(s): 61.50.Ks, 62.50.+p, 71.20.-b

INTRODUCTION

There is a considerable interest in producing metallic, and possibly superconducting, states of solid hydrogen at multi-megabar pressures (several hundred gigapascals).¹⁻³ Although solid hydrogen becomes opaque in visible light near 300 GPa, much higher pressures (e.g., >400 GPa) are thought to be needed for metallization, which currently are a great challenge for hydrogen with high-pressure techniques. It has been recently suggested that hydrogen-rich compounds such as CH₄, SiH₄, and GeH₄ will require pressures far less than expected for pure hydrogen at equivalent densities to enter metallic states.⁴ As is the case for pure hydrogen, these compounds are considered to be good candidates for high-temperature superconductors in their dense metallic forms.^{4,5} Hydrogen can be viewed in these systems as being “chemically precompressed,” which lowers the metallization pressure. While the conditions for forming metallic methane have not been reached experimentally,⁶ recent theoretical studies predict that both SiH₄ (Refs. 5 and 7) and GeH₄ (Ref. 8) transform to a metallic state at much lower and accessible pressures. However, there is only limited high-pressure experimental data available on these compounds, where an evidence for an insulator to semiconductor transition has been reported for solid silane (SiH₄) at pressures around 100 GPa from optical absorption and reflection measurements.⁹

At ambient pressures, solid CH₄, SiH₄, and GeH₄ consist of isolated high-symmetry tetrahedrally bonded molecules. For silane, two ambient pressure phases have been reported from the power x-ray diffraction, phase I forming on solidification below 88.5 K and phase II below 63.5 K. SiH₄ molecules form a noncubic crystal structure (probably with a tetragonal symmetry^{10,11}); however, the exact details could not be determined. Although several competitive crystal structures have been proposed for the high-pressure phases of silane in recent computational studies,^{5,7,12} there is a complete lack of reliable experimental data for its molecular and

crystal structure even at moderate pressures. Such information is important in understanding the changes in the electronic structure leading to metallization. In this paper, we report the crystal and molecular structure of solid silane at high pressures from a combined study using synchrotron x-ray diffraction and first-principles calculations.

EXPERIMENTAL AND COMPUTATIONAL DETAILS

Electronic grade (99.998+ %) silane (SiH₄) from Aldrich was used without further purification. Loading was done cryogenically in a dry nitrogen purged glove box by pre-cooling the diamond anvil cell (DAC) in a liquid nitrogen bath. Temperature was measured by a thermocouple attached to the DAC. SiH₄ solidified on the cooled rhenium gasket of the cell once the temperature of the cell body was a few degrees lower than the melting point of SiH₄ (88 K). The cell was then sealed and the solid SiH₄ was pressurized before warming up to room temperature. The entire loading process was monitored through an optical microscope mounted on the glove box. A ruby chip was inserted into an empty gasket prior to the loading of silane for pressure measurement. The pressure was determined from the shift of the R_1 ruby fluorescence line with an accuracy of $\pm 0.05 \text{ GPa}$ under quasihydrostatic conditions using the ruby scale from Ref. 13. After the loading was complete, the pressure was measured 11.3 GPa. Powder x-ray diffraction data were collected at beam line 16-ID-B (HPCAT) at the Advanced Photon Source. A focused monochromatic beam with wavelength $\lambda=0.3664 \text{ \AA}$ was used, and the data were recorded on a MAR image plate. The diffraction data were collected at room temperature from 11 to 40 GPa on pressure increase and down to 10 GPa on pressure decrease. Diffraction data were integrated azimuthally using FIT2D¹⁴ and structural information was obtained using JANA2000.¹⁵

Theoretical calculations were performed within the framework of density functional theory,^{16,17} as implemented by the

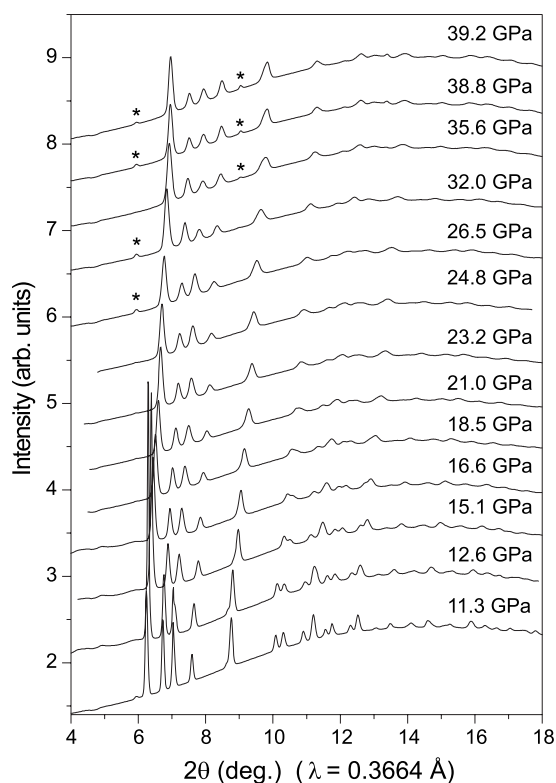


FIG. 1. X-ray diffraction patterns of solid SiH_4 at selected pressures. Asterisks denote additional peaks appearing above 25 GPa.

VASP package.^{18,19} The Perdew-Burke-Ernzerhof generalized gradient approximation²⁰ has been used for the exchange-correlation functional and, additionally, the all-electron problem has been simplified by means of ultrasoft pseudopotentials.²¹ Plane waves have been chosen as the basis set, and several structures have been studied in the pressure range of interest. For each structure and for every volume, both the lattice parameters and the atomic positions have been optimized via a two step process: Parameters are preoptimized via a low precision relaxation, and this is followed by a high precision relaxation. The final energy has been obtained in a static calculation using a $10 \times 10 \times 10$ Monkhorst-Pack²² grid and a 600 eV cutoff. It should be noted that in cases with large length differences between lattice vectors, the grid has been modified accordingly.

III. RESULTS AND DISCUSSION

X-ray diffraction of silane at 11.3 GPa revealed a high quality pattern with numerous reflections (Fig. 1). At these conditions, phase V of silane is stable, as found by our Raman and infrared measurements, while silane solidifies at 4 GPa, phase III exists in a narrow pressure range from 4 to 6.5 GPa, and phase IV is stable from 6.5 to 10 GPa.²³ With pressure increase, the diffraction peaks become significantly broader, but the diffraction pattern does not change significantly. Above 25 GPa, additional peaks appear (Fig. 1), which signals a phase transformation. The transition pressure of 25 GPa is in agreement with that obtained in our optical measurements.²³

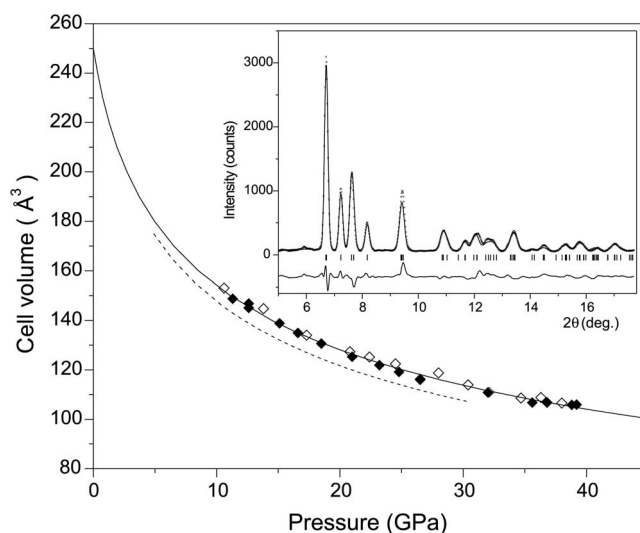


FIG. 2. Pressure dependence of the unit cell volume of the SiH_4 phase V. Solid and open symbols show data collected on pressure increase and pressure decrease, respectively. Solid and dashed lines represent the experimental and theoretical equations of state. Inset: integrated profile of the SiH_4 phase V at 24.8 GPa collected on pressure increase (crosses) and the Rietveld refinement fit for the $P2_1/c$ structure (line). The tick marks below the profile show the calculated peak positions. The lower curve is the difference between the observed and calculated profiles.

Phase V of silane is indexed with a monoclinic cell with lattice parameters $a=6.161(1)$ Å, $b=4.0722(2)$ Å, $c=6.122(1)$ Å, and $\beta=104.36(1)^\circ$ at 11.3 GPa, giving a unit cell volume of $148.78(1)$ Å³ at this pressure. All diffraction patterns up to 25 GPa could be indexed with this unit cell. Above this pressure, when the additional peaks appear, all the diffraction peaks, except the additional peaks, could still be fitted with the monoclinic cell. This indicates that above 25 GPa, the structure of phase V either becomes more complex or coexists with an appearing new high-pressure phase. The fit of the pressure dependence of the unit cell volume for phase V (Fig. 2) with the Birch-Murnaghan equation of state gives the following parameters at ambient pressure: $V_0=250(9)$ Å³ and $K_0=7.8(9)$ GPa with $K'_0=4$ assumed. The estimation using the ambient volume of the SiH_4 molecule of 73 Å³ gives four molecules in the unit cell. The space group is determined as $P2_1/c$ (No. 14). Phase V of SiH_4 appears to be isostructural with SnBr_4 and shares this structure type with several tetrahalides, where the Si atom is tetrahedrally coordinated by four hydrogen atoms (Fig. 3). Table I summarizes structural characteristics of known SnBr_4 -type phases in comparison to SiH_4 V.^{24–30} The b/a and c/a ratios of the SiH_4 V structure fall within the margins of the axial ratios of the other SnBr_4 -type structures. The β angle of the monoclinic unit cell takes a value of 102.2° – 104.4° for all the observed structures and is virtually pressure independent for the SiH_4 V structure.

The experimental diffraction pattern at 24.8 GPa was fitted on the basis of the $P2_1/c$ structure with Si atoms placed in the $4e$ position (0.249, 0.581, 0.371) and hydrogen atoms at $4e$ (0.036, 0.571, 0.158), $4e$ (0.325, 0.946, 0.434), $4e$ (0.453, 0.396, 0.300), and $4e$ (0.186, 0.395, 0.574) positions, as

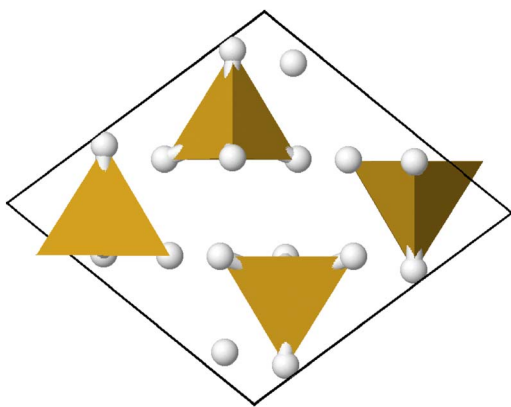


FIG. 3. (Color online) Calculated molecular and crystal structures for the SiH₄ phase V at 24 GPa, shown along the b axis.

obtained from our *ab initio* calculations. As can be seen in Fig. 2 (inset), the positions and intensities of the diffraction peaks of the SiH₄ V are fitted well within the proposed structures. The resulting R factors from the Rietveld refinement are $R_p=12.7\%$ and $R_{wp}=9.9\%$. Although the diffraction rings appeared to be relatively smooth, a strong preferred orientation was present. The March-Dollase preferred orientation model has been used to fit the diffraction pattern, which gave the best fit in the $[0, 1, -1]$ direction. The refined lattice parameters at this pressure are $a=5.699(1)$ Å, $b=3.814(1)$ Å, $c=5.643(1)$ Å, and $\beta=104.38(1)^\circ$.

The stability of the SiH₄ V structure is confirmed by our *ab initio* calculations. According to these (Fig. 4), in the pressure range from 2 to 27 GPa the monoclinic $P2_1/c$ structure is favored over other molecular solids [with SiH₄ molecules packed in bcc (GeF₄-type), simple cubic, and fcc (CH₄-type) arrangements considered in a recent theoretical work⁵]. It is also more stable than the $Pmna$ structure suggested by Feng *et al.*⁵ and the $P2/c$ structure proposed by Pickard and Needs.⁷ As shown in Table I, a very good

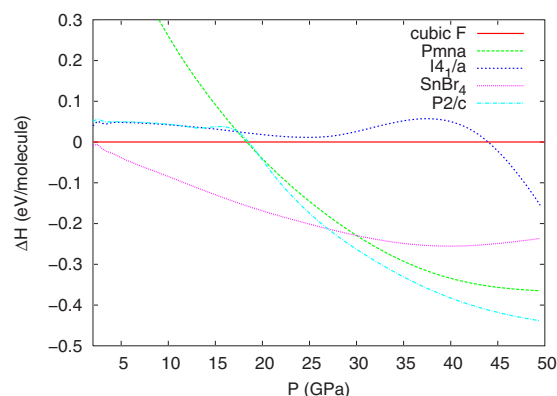


FIG. 4. (Color online) Enthalpy evolution with pressure of the relevant structures of SiH₄ considered here. The enthalpy of the face-centered-cubic structure is used as a reference.

agreement between calculated and measured structural parameters defining the SiH₄ V structure is also obtained. Additionally, the calculated compressibility of the $P2_1/c$ phase agrees well with experiment. Fixing K'_0 to 4 and fitting only calculated data of SiH₄ V between 5 and 27 GPa to a Birch-Murnaghan equation of state gives $V_0=255(\pm 2)$ Å³ and $K_0=6.1(\pm 2)$ GPa. This result compares well with the experimental equation of state (Fig. 2), considering the approximations made for molecular crystals.

Ab initio calculations of the evolution of the Si-H distance with pressure provide additional insight into the modification of its bonding properties. At ambient pressure, the Si-H bond length in the $P2_1/c$ structure is 1.488 Å, which is identical to that of the free molecule. With increasing pressure, this distance decreases, though perhaps not as much as expected. At 27 GPa, although the volume has suffered a 2.4-fold reduction, corresponding to a 1.34 factor in linear dimensions, the Si-H distance is still 1.466 Å (a reduction of only 1.5%). On the other hand, the six H-Si-H angles in the tetrahedra range between 107.3° and 111.8°, which is close to the correspond-

TABLE I. Structural characteristics of SiH₄ phase V compared with those of tetrahalides with the SnBr₄-type structure.

Phase	P, T	a (Å)	b (Å)	c (Å)	β (deg)	b/a	c/a	Ref.
SnBr ₄	293 K	10.59(3)	7.10(2)	10.66(3)	103.6(2)	0.670	1.007	24
TiBr ₄	293 K	10.17(2)	7.09(1)	10.41(1)	102.0(2)	0.697	1.024	25
TiCl ₄	241 K	9.70	6.48	9.75	102.67	0.668	1.005	26
SnCl ₄	234 K	9.85	6.75	9.98	102.25	0.685	1.013	26 and 27
SiCl ₄	163 K	9.608(4)	6.356(2)	9.672(4)	102.91	0.661	1.007	28
CCl ₄ III	1 GPa, 300 K	9.08(2)	5.764(3)	9.201(3)	104.29(5)	0.635	1.013	29
CF ₄ III	6.2 GPa, 300 K	6.776	4.423	6.818	102.97	0.653	1.006	30
SiH ₄ V	11.3 GPa, 300 K	6.122(1)	4.0722(2)	6.161(1)	104.36(1)	0.661	1.006	Expt.
SiH ₄ V	11.6 GPa, 0 K	6.012	4.033	6.042	104.28	0.670	1.005	Theory

ing angle in a regular tetrahedron (109.47°). Additionally, the band gap decreases rapidly on compression from 6.36 eV at ambient pressure to 2.86 eV at 27 GPa. All these features indicate the prevalence of repulsive intermolecular forces in silane under these conditions and that below 27 GPa silane is an insulating molecular solid.

Figure 4 shows that with increasing pressure, both the $P2_1/c$ structure⁷ and the $Pmna$ structure⁵ are favored over $P2_1/c$. Remarkable differences arise when these structures are compared with SiH_4 V ($P2_1/c$). The $P2_1/c$ structure is characterized by zigzag chains of H-bonded Si atoms along the c axis, while the $Pmna$ structure can be described as sheets of octahedrally coordinated Si atoms sandwiched between layers formed by H double sheets. Therefore, around 27 GPa covalentlike structures with a higher coordination number begin to be preferred over $P2_1/c$. However, we remark that the observed x-ray diffraction pattern above 27 GPa (Fig. 1) cannot be reproduced considering either $P2_1/c$ nor $Pmna$ structures with the atomic positions obtained from *ab initio* calculations. The observed diffraction patterns indicate that SiH_4 transforms to a new structure in this pressure range. In this regime, major changes in electronic properties are predicted.⁵

In conclusion, the crystal structure of SiH_4 between 10 and 25 GPa has been solved from powder diffraction data and confirmed by *ab initio* calculations. In this pressure range, SiH_4 is found to be a molecular insulator with a

monoclinic unit cell containing four tetrahedrally bonded molecules (space group $P2_1/c$). The x-ray diffraction patterns observed above 27 GPa are more complex than predicted by the $P2_1/c$ structure and are not compatible with either $P2_1/c$ or $Pmna$ structures. Further experimental and theoretical work is underway to investigate the higher-pressure phases.

ACKNOWLEDGMENTS

The authors thank H. P. Liermann for his help with experiments. This work was supported by NSF (DMR), DOE Grant No. DEFG02-02ER4595, and DOE (CDAC). The x-ray measurements were performed at HPCAT (Sector 16), Advanced Photon Source (APS), Argonne National Laboratory. The HPCAT facility is supported by DOE-BES, DOE-NNSA (CDAC), NSF, DOD-TACOM, and the W.M. Keck Foundation. The use of the APS was supported by DOE-BES under Contract No. W-31-109-ENG-38. M.M.C. would like to thank the Spanish Ministry of Education and Science for providing a grant. M.M.C. and A.B. acknowledge partial support from the EC sixth Framework Network of Excellence NANOQUANTA (NMP4-CT-2004-500198). Computational resources for this work were provided by the SGI/IZO-SGIker at the UPV/EHU (supported by the Spanish Ministry of Education and Science and the European Social Fund).

*Present address: Department of Chemistry, The University of Western Ontario, London, Ontario Canada N6A 5B7.

¹A. F. Goncharov, E. Gregoryanz, R. J. Hemley, and H. K. Mao, Proc. Natl. Acad. Sci. U.S.A. **98**, 14234 (2001).

²P. Loubeyre, F. Occelli, and R. LeToullec, Nature (London) **416**, 613 (2002); see also H. K. Mao and R. J. Hemley, Science **244**, 1462 (1989).

³C. Narayana, H. Luo, J. Orloff, and A. L. Ruoff, Nature (London) **393**, 46 (1998).

⁴N. W. Ashcroft, Phys. Rev. Lett. **92**, 187002 (2004).

⁵J. Feng, W. Grochala, T. Jaron, R. Hoffmann, A. Bergara, and N. W. Ashcroft, Phys. Rev. Lett. **96**, 017006 (2006).

⁶M. Martinez-Canales and A. Bergara, High Press. Res. **26**, 369 (2006); L. Sun, A. L. Ruoff, C.-S. Zha, and G. Stupian, J. Phys. Chem. Solids **67**, 2603 (2006).

⁷C. J. Pickard and R. J. Needs, Phys. Rev. Lett. **97**, 045504 (2006).

⁸M. Martinez-Canales, A. Bergara, J. Feng, and W. Grochala, J. Phys. Chem. Solids **67**, 2095 (2006).

⁹L. Sun, A. L. Ruoff, C.-S. Zha, and G. Stupian, J. Phys.: Condens. Matter **18**, 8573 (2006).

¹⁰W. M. Sears and J. A. Morrison, J. Chem. Phys. **62**, 2736 (1975).

¹¹E. Legrand and W. Press, Solid State Commun. **18**, 1353 (1976).

¹²Y. Yao, J. S. Tse, Y. Ma, and K. Tanaka, Europhys. Lett. **78**, 37003 (2007).

¹³H. K. Mao, J. Xu, and P. M. Bell, J. Geophys. Res. **91**, 4673 (1986).

¹⁴A. P. Hammersley, S. O. Svensson, M. Hanfland, A. N. Fitch, and D. Hausermann, High Press. Res. **14**, 235 (1996).

¹⁵V. Petricek, M. Dusek, and L. Palatinus, *The Crystallographic Computing System JANA2000* (Institute of Physics, Praha, Czech Republic, 2000).

¹⁶P. Hohenberg and W. Kohn, Phys. Rev. **136**, B864 (1964).

¹⁷W. Kohn and L. J. Sham, Phys. Rev. **140**, A1133 (1965).

¹⁸G. Kresse and J. Hafner, Phys. Rev. B **47**, 558 (1993).

¹⁹G. Kresse and J. Furthmüller, Phys. Rev. B **54**, 11169 (1996).

²⁰J. P. Perdew, K. Burke, and M. Ernzerhof, Phys. Rev. Lett. **77**, 3865 (1996).

²¹D. Vanderbilt, Phys. Rev. B **41**, 7892 (1990).

²²H. J. Monkhorst and J. D. Pack, Phys. Rev. B **13**, 5188 (1976).

²³X. J. Chen, V. V. Struzhkin, Y. Song, A. Goncharov, M. Ahart, Z. X. Liu, H. K. Mao, and R. J. Hemley (unpublished).

²⁴P. Brand and H. Sackmann, Acta Crystallogr. **16**, 446 (1963).

²⁵P. Brand and J. Schmidt, Z. Anorg. Allg. Chem. **348**, 257 (1966).

²⁶P. Brand and H. Sackmann, Z. Anorg. Allg. Chem. **321**, 262 (1963).

²⁷H. Reuter and R. Pawlak, Z. Anorg. Allg. Chem. **626**, 925 (2000).

²⁸L. N. Zakharov, M. Yu. Antipin, Yu. T. Struchkov, A. V. Gusev, A. M. Gibin, and N. V. Zhernenkov, Sov. Phys. Crystallogr. **31**, 99 (1986).

²⁹G. J. Piermarini and A. B. Braun, J. Chem. Phys. **58**, 1974 (1973).

³⁰D. Shindo, T. Yoshii, Y. Akahama, and H. Kawamura, J. Phys.: Condens. Matter **14**, 10653 (2002).